ORNL/TM-11197

OAK RIDGE NATIONAL LABORATORY

MARTIN MARIETTA

Characterization of Fiber-Reinforced Particulate Filters

D. P. Stinton
L. Riester
D. Dellinger

Research Supported
by the
Morgantown Energy Technology Center,
U.S. Department of Energy

Fossil Energy Program

OPERATED BY
MARTIN MARIETTA ENERGY SYSTEMS, INC.
FOR THE UNITED STATES
DEPARTMENT OF ENERGY

ORNL/TM-11197

Metals and Ceramics Division

CHARACTERIZATION OF FIBER-REINFORCED PARTICULATE FILTERS

D. P. Stinton
L. Riester
D. Dellinger

Date Published: May 1989

NOTICE: This document contains information of a preliminary nature. It is subject to revision or correction and therefore does not represent a final report.

Prepared for the
DOE Office of Fossil Energy
(AA 05 10 00 0)

Prepared by the
OAK RIDGE NATIONAL LABORATORY
Oak Ridge, Tennessee 37831-6285
operated by
MARTIN MARIETTA ENERGY SYSTEMS, INC.
for the
U.S. DEPARTMENT OF ENERGY
under contract DE-AC05-84OR21400

CONTENTS

LIST OF FIGURES v
ABSTRACT 1
INTRODUCTION 1
EXPERIMENTAL PROCEDURE 8
RESULTS AND DISCUSSION 13
CONCLUSIONS 26
ACKNOWLEDGMENTS 27
REFERENCES 28

LIST OF FIGURES

Fig. 1. Candle filter assembly illustrating simultaneous filtering and cleaning of the candles 2

Fig. 2. Schematic illustrating the operation of a crossflow filter element 3

Fig. 3. Schematic showing the process for fabricating tubular fiber-reinforced filters 9

Fig. 4. Schematic showing the process for fabricating disk-shaped filter specimens 10

Fig. 5. Apparatus used for mechanical strength testing of fiber-reinforced filters 11

Fig. 6. Equipment used for thermal shock testing of filters . . . 12

Fig. 7. The desired microstructure for a coated filter. Coatings would be quite smooth because the grain size would be extremely small. Fine grains would result in better strengths 14

Fig. 8. Microstructure of typical filters showing nodular appearance of the coating; (*a*) and (*b*) nodular coating where individual agglomerates have not grown together, and (*c*) and (*d*) nodular coating where agglomerates have grown together to form a smoother coating 16

Fig. 9. Strength test results of a lightly coated filter 18

Fig. 10. Strength test results of a heavily coated filter 19

Fig. 11. Strength test results for appropriately coated filter 20

Fig. 12. Scanning electron micrograph showing a failed filter with cracked coatings but intact fibers 21

Fig. 13. Schematic drawing of a corrugated candle filter 24

Fig. 14. Effect of pressure cycling on disk-shaped filter specimens 25

CHARACTERIZATION OF FIBER-REINFORCED PARTICULATE FILTERS*

D. P. Stinton, L. Riester, and D. Dellinger

ABSTRACT

Fiber-reinforced particulate filters for high-temperature application were fabricated by a recently developed chemical vapor deposition process. Mechanical property testing of these filters revealed that fibrous materials required coating with 2 to 5 μm of silicon carbide to produce acceptable strengths and thermal shock resistance. Thinner coatings were very weak and resulted in unacceptable flexing of the filters. Thicker coatings were very strong but resulted in brittle fracture of the filters. Appropriately coated filters had both an acceptable strength and the improved damage tolerance required of particulate filters. Thermal shock and repeated pressure cycling representative of pressure pulse cleaning had no apparent effect on the burst strength of filter specimens.

INTRODUCTION

Particulate filters that operate at temperatures up to 1300 K will be required for cost-effective operation of advanced coal conversion systems. Processes of particular interest include direct combustion of coal in a pressurized, fluidized-bed combustor (PFBC), and coal gasification. New technologies that will require hot-gas cleanup devices include coal-fired gas turbines and coal-fired diesel engines. In these systems, contaminants such as sulfur, alkalies, NO_x, and solid particulates must be removed from the gas stream to protect metallic turbine or engine components from corrosion and erosion. Commercially proven particulate removal techniques are available; however, the requirement that the gas be cooled prior to entering the filter results in reduced system efficiency.

*Research sponsored by the U.S. Department of Energy, Morgantown Energy Technology Center, under contract DE-AC05-84OR21400 with Martin Marietta Energy Systems, Inc.

To maintain high gas temperatures, three types of ceramic filters are being developed for coal conversion systems: candle, crossflow, and fabric. Candle filters are fabricated by bonding silicon carbide grains with a clay binder to form a porous tube 8 cm in diameter, 1.5 m long, and 2 cm wall thickness. Various types of fibers are sometimes incorporated into the binder to reduce the size of the pores on the filter surface. Particulate-laden gases enter a filter assembly that contains many candles and pass from the outside of the candles to the inside, with the particulates trapped on the outer surface of the candles (Fig. 1). The filter is cleaned by periodically reversing the flow of gas to remove the dustcake and prevent the formation of a significant pressure drop across the thickness of the filter. Candle filters are attached to a metallic tubesheet such that cleaned gases are collected in a gas plenum and sent to a turbine.

ORNL-DWG 88-10424

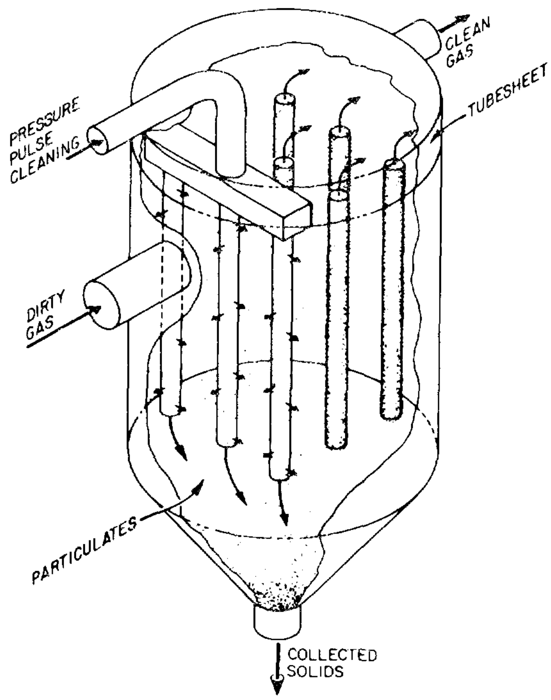

Fig. 1. Candle filter assembly illustrating simultaneous filtering and cleaning of the candles.

Crossflow filters under development at Westinghouse, Coors Porcelain Company, and elsewhere appear promising because they are compact and offer much greater surface area than candle filters. Crossflow filters are fabricated by sintering together multiple sheets of extruded cordierite or a mixture of mullite, cordierite, and alumina (Fig. 2). Each layer is corrugated and consists of rectangular grooves with porous sides and bottom. The layers are offset at 90° so that dirty gas which enters the shorter channels permeates the floor and roof of the channels, then enters the long clean channels where the filtered gas exits the element. The dustcake is deposited on the filter surfaces within the dirty channels and must be periodically removed by a reverse pulse of cleaning gas that flows down the clean channels through the porous barriers, lifting off the dust deposit and expelling the dustcake from the unit. As with the candle filters, the clean side channels are manifolded to a gas plenum where they exit to the turbine.

ORNL-DWG 89-8946

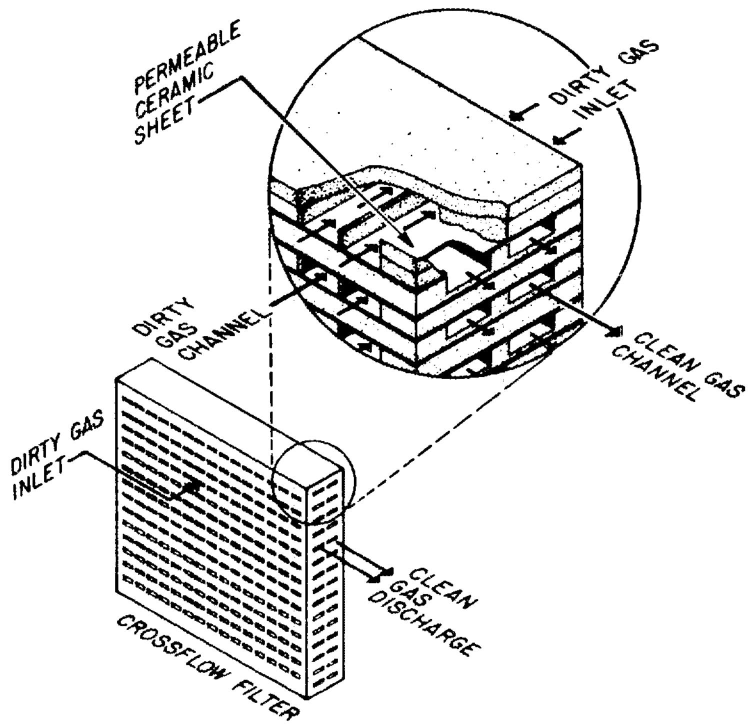

Fig. 2. Schematic illustrating the operation of a crossflow filter element.

Ceramic fibers formed into a mat or woven cloth are fabricated into flexible bag filters. Fabric filters, particularly those fabricated from mats, are very weak and must be supported by metallic webs or screens. The fibrous materials most often used for particulate filtration include aluminosilicates, silicon carbide, and zirconia. Bag filters are configured like candle filters and cleaned by a periodic reverse pulse of cleaning gas. Flexing of the bag filter assists in removing the dustcake from the filter surface.

Unfortunately, each of these types of filters has serious limitations which prevent their use in coal conversion systems.[1] Economically viable filters must be sufficiently durable to function without failure for at least one year of continuous operation; however, current filters can endure only several hundred hours of operation. Candle filters fail because they are susceptible to brittle fracture.[1] Mechanical stresses, particularly at the flange near the tubesheet, and thermal stresses due to reverse pulsing with cool cleaning gas often exceed the mechanical strength of the material. In addition, the clay binder used to bond the SiC grains together eventually forms a glass matrix that is easily damaged by thermal shock. Brittle fracture of the candles causes the lower section to drop to the bottom of the assembly. Catastrophic failure of the candles results in a large fraction of the contaminated gas passing through the broken filter and directly to the turbine. Significant quantities of particulates passing through the turbine will cause severe damage in a very short time. Ceramic crossflow filters are also very susceptible to thermal shock and brittle failure.[1] Mechanical stresses near the flange and thermal stresses within each layer often result in stresses sufficiently large to cause delamination of the weakly bonded layers. As with candle filters, catastrophic failure of crossflow filters results in severe damage to the turbine. In addition, permeability of the floors and roofs of the channels within crossflow filters may decrease after extended periods, resulting in large pressure drops.

The porous nature of flexible fabric filters and the use of low-modulus continuous fibers make them very resistant to thermal shock damage. However, the strength of the fibers are easily degraded by rough handling of the fabrics, excessive temperatures, or corrosion.[2] Filter bag failures occur frequently if excessive clamping forces are used at the tubesheet, or if the fabric is folded during installation or use.[1] Fabrics are not of high purity and cannot be used at high temperatures or where halides are present. The most frequently observed type of failure, however, is referred to as pinholing.[1] Since fibers are free to move within the felt or weave, pinholes can form that decrease the filtering efficiency of the material.

An additional problem with all of these filters is their susceptibility to corrosion by alkali metals and possibly steam. Since current filters fail mechanically after only several hundred hours of exposure testing, the significance of the corrosion problem is yet to be realized by many researchers. Improved designs for candle and crossflow filters will eliminate significant mechanical stresses at flanges and corners, and the filters should survive for much longer periods of time. During long-term testing of improved filter designs, corrosion of the filter materials will become a much more significant issue. In recent work at NASA Lewis Research Center, Cleveland, Ohio, and at ORNL, sodium and potassium were shown to cause severe corrosion of SiC and Si_3N_4 turbine engine components at temperatures above 1200°C.[3-6] In addition, there is evidence of steam corrosion of SiC refractories at temperatures below 1000°C.[7] Therefore, the SiC candle filters may be susceptible to sodium and steam corrosion should they be modified sufficiently to survive thermal shock. Unfortunately, alumina and cordierite ($3Al_2O_3 \cdot 2MgO \cdot 5SiO_2$) used in crossflow filters are also susceptible to corrosion by sodium. Alumina undergoes a destructive phase transformation that occurs in the presence of sodium.[8] The phase change results in a 15% volume expansion that spalls the surface layer and decreases the strength of the material. In cordierite, magnesia is gradually leached out of the material.[9]

The SiC and Si_3N_4 materials evaluated in sodium corrosion tests at NASA Lewis and ORNL contained 5 to 10% sintering aids that concentrated at grain boundaries. Thus, corrosion of these materials may be due to attack of the grain boundary phases. The SiC refractories corroded by steam consisted of SiC grains bonded by a clay (or Si_3N_4) matrix, and corrosion of this material may result because of degradation of the binder phase rather than the SiC grains. It is therefore premature to believe that SiC is unacceptable for this application because high-purity SiC without grain boundary contamination may be sufficiently inert to survive.

A new approach to high-temperature particulate filtration utilizing fiber-reinforced composite technology has been developed at ORNL which overcomes the problems mentioned above and offers several advantages.[10] These fiber-reinforced particulate filters consist of a mat or felt of continuous ceramic fibers overcoated with a ceramic matrix to provide the necessary strength, damage tolerance, and corrosion resistance. Strength is achieved because the ceramic coating bonds fibers together at crossover points and rigidifies the material. Since fibers are locked together at crossover points, they are no longer free to move and create pinholes that result in the low filtering efficiencies seen in fabric filters. Damage tolerance is used here to qualitatively describe the capacity of the material to withstand local overstress without catastrophic failure. Damage tolerance is high in these composite materials for several reasons. First, the felts or fabrics are very porous and overcoating does not significantly decrease the porosity. Pores act to blunt cracks, making the material much more resistant to brittle failure.[11] A second, and more significant, reason for the improved damage tolerance is the use of low modulus continuous fibers. Since the fibers are much more elastic than the ceramic overcoat, and because the coating-fiber bond can be controlled, slippage of fibers in the coating can absorb energy to prevent the propagation of cracks.[12] That is, the material behaves much like a high-temperature fiberglass composite; when the matrix fractures the fibers remain intact to carry the load.

Another advantage of the fiber-reinforced filter approach is the potential improvement in corrosion resistance of chemically vapor deposited materials. Silicon carbide, which can be applied at temperatures that will not damage Nicalon or Nextel fibers, was selected as the coating material. The high purity of SiC offered by the chemical vapor deposition route may be sufficiently resistant to sodium and steam corrosion at temperatures below 1300 K. However, it is possible that sodium or steam can corrode even the purest SiC, and alternate materials shall be selected with which to overcoat fibrous materials for filter applications. Two materials,

$Na_2O \cdot 11Al_2O_3$ and mullite, which appear to have improved corrosion resistance are currently being investigated.

An advantage of fiber-reinforced filters over ceramic bag filters is their strength and rigidity. Bag filters have very little strength and therefore must be supported by a metallic cage or screen. The metallic components, of course, limit the operating temperature of the filter. The ceramic overcoat of fiber-reinforced filters, however, provides sufficient strength for the filter, eliminating the need for metallic supports.

A final advantage of the fiber-reinforced filter approach over conventional candle filters is their light weight. Conventional candle filters are quite heavy (11 kg or 25 lb), and therefore it is difficult to find a metallic tubesheet material with sufficient strength at the elevated temperature to support the weight of many (50 or more) filter elements. The fiber-reinforced filter materials are very porous and less than 0.5 cm thick; therefore, they are very light (<2 kg) and the selection of a tubesheet material should be much easier.

The strength requirements of candle filters are actually quite modest since filters must support only their own weight and the weight of the dustcake, and withstand a pressure drop of about 20 KPa (3 psi) during both the filtering and cleaning cycles. However, the requirements for thermal shock resistance and resistance to cyclic fatigue are significantly more stringent. Candle filters operate at about 1200 K and must be cleaned approximately 2 to 20 times each hour throughout their life.[13] The cleaning cycle consists of shutting off the flow of particulate-laden gases to one bank of candles and backflushing with a very short blast (1 s) of air from a pressurized reservoir (pressure drop across the filter is about 20 KPa). The thermal stresses created by backflushing with low-temperature air are quite significant and result in multiple thermal shocks of 300 to 500 K each cycle. The repeated filtering and cleaning cycles result in alternating compressive and tensile stresses that could cause cyclic fatigue failure of the candles. The objective of the current work is to characterize fiber-reinforced filters for burst strength and evaluate their resistance to thermal shock and cyclic fatigue damage.

EXPERIMENTAL PROCEDURE

High-temperature particulate filters are fabricated at ORNL by a chemical vapor deposition process.[10] This process places a freestanding fibrous material (Nicalon* felt) within a constant temperature region (1400 K) of a resistively heated deposition furnace and deposits SiC on and around each of the fibers making up the felt. Initially, a dilute mixture of propylene and argon is forced through the fibrous preform to deposit a thin layer (0.2 μm) of carbon. The thin layer of pyrolytic carbon serves two functions: (1) to protect the fibers from chlorides produced during silicon carbide deposition, and (2) to provide appropriate fiber-matrix bonding for fiber pullout and toughening.[14-16] Deposition of a thin layer (1 to 5 μm) of silicon carbide then occurs by a similar process using methyltrichlorosilane (MTS or CH_3SiCl_3) and hydrogen at 1400 K and about 5 KPa of pressure. The MTS decomposes at high temperatures in the presence of hydrogen to deposit SiC and release HCl. MTS is preferred over other reactants because it deposits stoichiometric SiC over a wide range of operating conditions. The deposited SiC serves to bond the fibers together, provides the necessary mechanical strength, and prevents fiber movement or loss during pressure pulse cleaning. The process has been developed to the extent that SiC is uniformly deposited across the diameter and thickness of the felt.

Industrial-scale candle filters are fabricated from SiC in the shape of tubes ~8 cm in diameter and 1.5 m long. For demonstration purposes, model fiber-reinforced tubular filters (6 cm in diameter, 15 cm long, and 0.3 cm thick) have been fabricated at ORNL using the process shown schematically in Fig. 3. A tubular preform consisting of Nicalon felt is placed in an isothermal hot zone of a furnace. Reactant gases are injected into the center of the tube and forced through the walls where deposition occurs, and effluents exit through the top of the furnace.

Mechanical property characterization was initiated by attempts to measure the burst strength of the fiber-reinforced material. Characterization techniques that inflate a rubber bladder to stress a

---

*SiC fibers fabricated by Nippon Carbon Co., Tokyo, Japan.

ORNL-DWG 88-5940

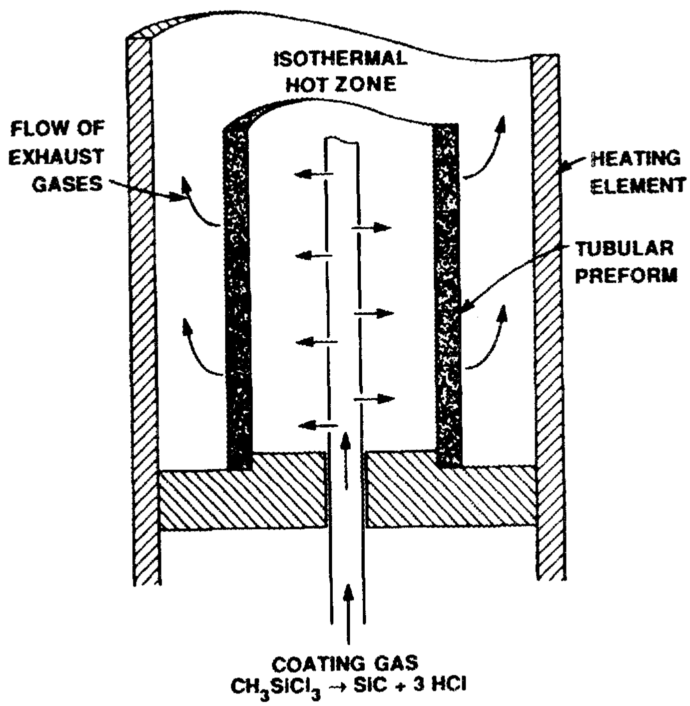

Fig. 3. Schematic showing the process for fabricating tubular fiber-reinforced filters.

tubular filter were unacceptable because the slight flexing normally exhibited by fiber-reinforced materials would be detected as failure (change in volume of the fluid-filled bladder). Furthermore, detection of failure by displacement of the filter surface would be impossible because of the large surface area of the tubular filter. Therefore, to enable use of displacement techniques, small flat filter disks were fabricated for testing which were about 5 cm in diameter and 0.3 cm thick. The burst strength of the filter disk was defined as the pressure required to cause excessive displacement at the center of the filter disk. Excessive displacement occurred when the slope of the pressure-displacement curve was equal to the slope of an unsupported rubber bladder. The burst strength is a relative measure of the filter's strength to be used only to compare the strength of filter disks fabricated using different processing conditions. It is not clear how the burst strength compares to the pressure drop experienced by actual filters.

The equipment used to fabricate the disk-shaped filters is shown in Fig. 4. Two filter disks were fabricated simultaneously with coating gases forced through a graphite inlet tube into the center of a short graphite cylinder oriented perpendicular to the inlet tube. A filter specimen is mounted at each end of the cylinder and held in place by a retaining ring. The gases flow into the cylindrical specimen holder and are forced through the disk-shaped filter specimens, where deposition of SiC occurs.

A series of ~60 filter specimens was fabricated for burst-strength testing. The experimental conditions utilized to fabricate the filters were identified in a designed series of experiments investigating deposition temperature, MTS concentration, and total flow rate. Previously, the

ORNL-DWG 88-16174

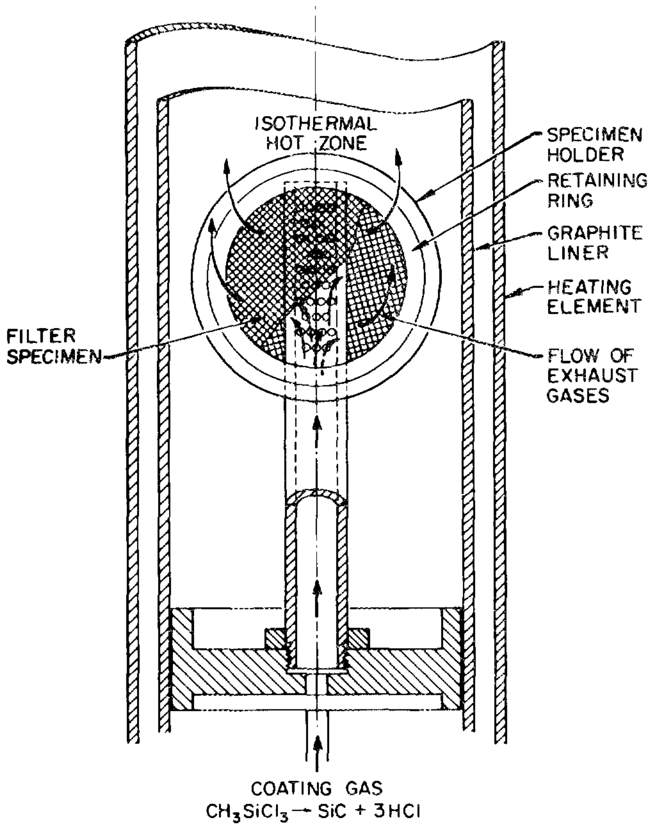

Fig. 4. Schematic showing the process for fabricating disk-shaped filter specimens.

SiC coatings deposited on Nicalon were very coarse grained and nodular. Results from the designed experiments indicated that reduced MTS concentrations and lower deposition temperatures produced the smoothest coatings. Conditions of 1400 K, 5 KPa total pressure, 5% MTS concentration, and a total flow rate of 525 cm^3/min (the best conditions identified to this point) were selected for this work; however, the coatings were still very nodular.

The mechanical strength of uniformly coated disk-shaped filter specimens was measured using equipment designed and fabricated at ORNL (Fig. 5). A neoprene diaphragm within the test fixture was placed against the filter and loaded with pressurized air. Careful control of the flow of pressurized air was achieved using a mass flow meter set at 100 cm^3/min, which insured that the loading rate was uniform throughout the test and from one test to another. Displacement of the neoprene diaphragm was

ORNL-DWG 88-15249R

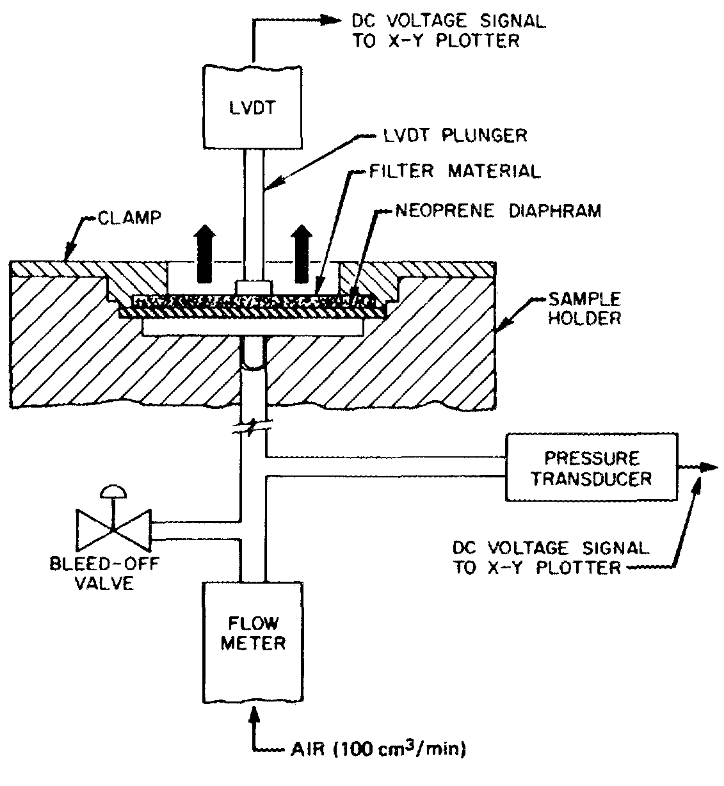

Fig. 5. Apparatus used for mechanical strength testing of fiber-reinforced filters.

restrained by the filter material until damage to the silicon carbide coating occurred. After the coatings begin to crack, the load is carried by the fibers and the filter flexes upward at the center. Displacement continues until the rate of displacement is equal to that of the neoprene disk alone, which indicates complete failure. Displacement is measured by a linear variable differential transformer (LVDT) placed against the top surface of the filter specimen which is connected to the Y axis of an X-Y recorder. Pressure monitoring was accomplished with a pressure transducer connected to a digital indicator and to the X axis of an X-Y recorder. For each strength test, pressure was plotted versus filter deflection.

Filter specimens were also characterized for thermal shock resistance. Filter disks were heated to 1100 K in an apparatus utilizing a propane torch and a simple blower (Fig. 6). After annealing the filter

ORNL-DWG 88-15250

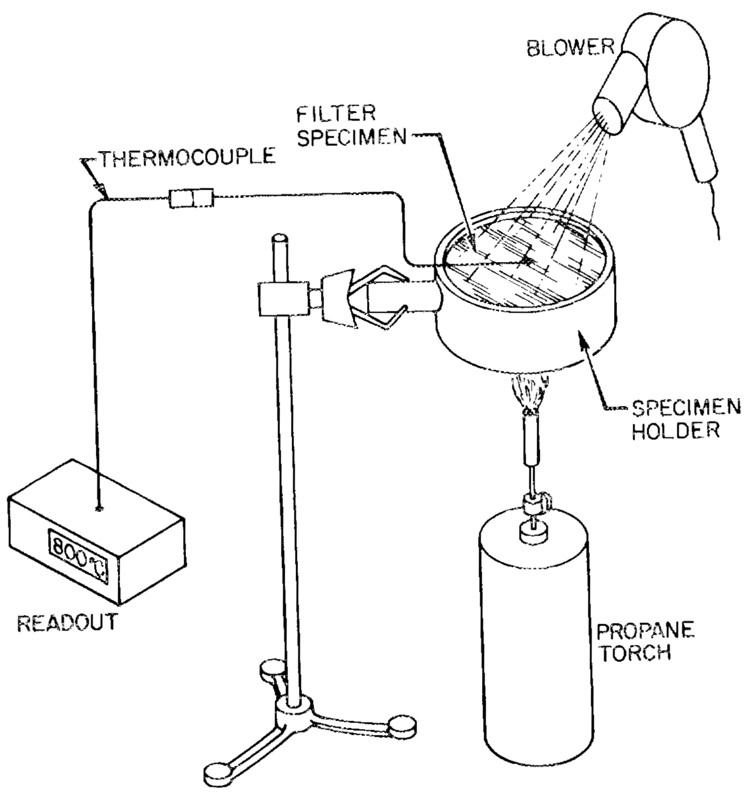

Fig. 6. Equipment used for thermal shock testing of filters.

specimens for 2 min, the propane torch was extinguished and the filter specimens were air-blast cooled using 500 K air. The heating-cooling cycle was repeated 20 or more times, and the filters were examined for cracks using a scanning electron microscope. A companion filter specimen fabricated in the same experimental run was then used in strength tests.

Characterization was completed by evaluating filter specimens after cyclic loading. Using the mechanical burst-strength testing apparatus, filter specimens were loaded to specific pressures insufficient to cause matrix cracking. After 1 min the pressure was relieved and the cycle repeated. Filter specimens were cycled 100 times and then strength tested using the burst technique. The effect of cyclic loading was also evaluated by strength-testing specimens loaded in a stepwise fashion until failure. For example, filters were loaded to a pressure of 13.7 KPa (2 psi) for a total of 20 cycles. The pressure was then increased to a loading of 17.2 KPa (2.5 psi) for an additional 20 cycles, and the process was continued at 2.4 KPa (0.5 psi) increments until failure of the filter occurred.

RESULTS AND DISCUSSION

During the first few months of this program, SiC coatings were deposited directly onto Nicalon fibers. These coatings were smooth and consisted of very fine grains. However, testing of these filters at Acurex Corporation* revealed that the strength of the Nicalon fibers decreased significantly during deposition of the SiC coating. Degradation of the Nicalon resulted in filters that were somewhat brittle, failing around the outer edge.[17] Therefore, the Nicalon fibers were subsequently precoated with pyrolytic carbon (PyC) to protect the fibers from the damaging SiC deposition conditions and produce an appropriate fiber-matrix bond. Various thicknesses of pyrocarbon were evaluated and 0.2 μm was determined to work well.[14] Thicknesses of at least 0.1 μm were required to protect the Nicalon from degradation during SiC processing, and thicknesses greater than 0.5 μm noticeably reduced the strength of the composite.

---

*Mountain View, California.

Smooth, fine-grained coatings are desired for the filter application for several reasons (Fig. 7). One of the primary functions of the ceramic overcoating is to protect the fibers from corrosive attack. Corrosion would occur by species diffusing through the coating and attacking the underlying fibers. Diffusion would occur through either the grains themselves or along the grain boundaries. Grain boundary diffusion is much

ORNL-PHOTO 3561-88

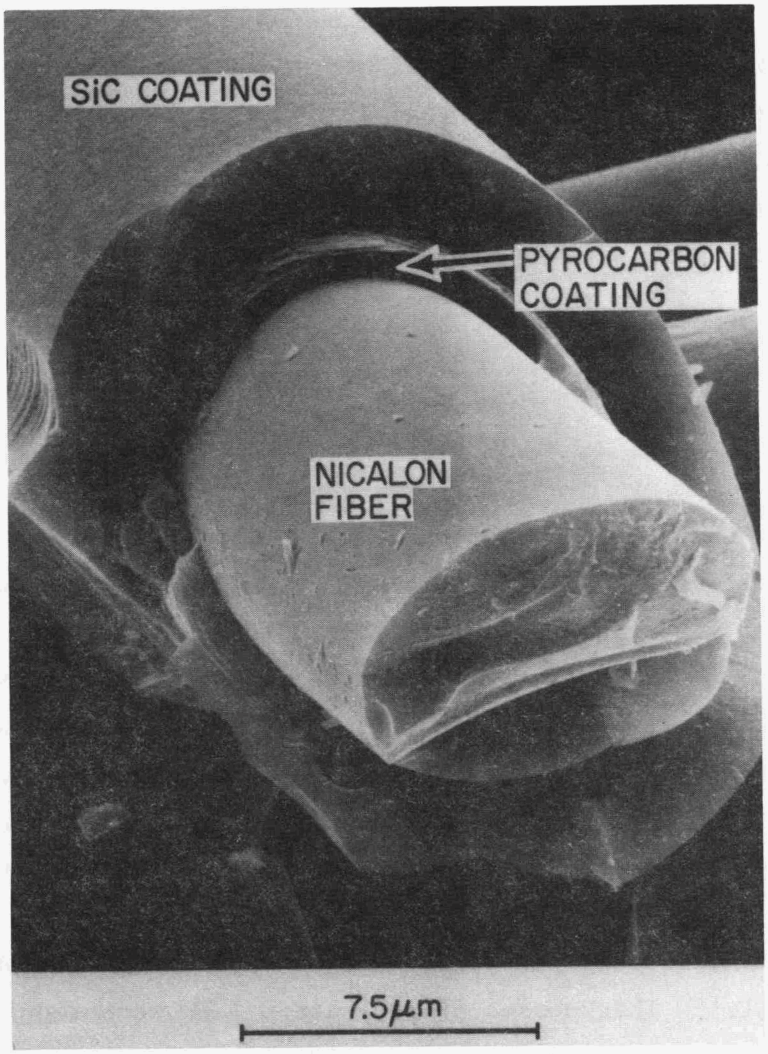

Fig. 7. The desired microstructure for a coated filter. Coatings would be quite smooth because the grain size would be extremely small. Fine grains would result in better strengths.

more rapid because of the lack of an ordered structure at the grain boundary. Therefore, for a given thickness, a fine-grained coating would present a much more tortuous path for diffusion than a coarse-grained coating. The second major function of the coating is to provide strength to the filter body. During ceramic processing of any type, fine-grained structures normally exhibit higher strengths than coarse-grained structures.[18] Therefore, fine-grained coatings are also desired for this application since the strength must be supplied by a very thin layer of coating.

In the chemical vapor deposition process, fine-grained coatings are achieved by assuring an ample supply of nucleation sites on the substrate surface and on the surface of the coating as it is being deposited.[19] Therefore, grain growth is prevented because nucleation sites are present to renucleate new grains. Unfortunately, this process seems to be disrupted by the PyC coating. Poor nucleation on the surface of the PyC surface results in very coarse, nodular coatings [Fig. 8(*a*,*b*)]. Two modifications were made to the deposition process to alter the PyC surface and enhance nucleation of SiC. Neither alternative was particularly successful in modifying the morphology of the coating; however, for future reference the modifications are described. The first attempt was to avoid a sharp PyC-SiC interface by gradually changing the composition of the interlayer from carbon to carbon plus SiC to pure SiC [Fig. 8(*c*,*d*)]. Coatings produced in this fashion were improved; however, they were still quite nodular and theoretically more susceptible to oxidation because of the increased amount of carbon. A second potential solution to enhance nucleation of SiC was the deposition of metallic silicon from silane onto the pyrocarbon. Pyrolytic carbon was, of course, still required to protect the Nicalon fibers and provide the appropriate fiber-coating bond. The deposited silicon will react with the carbon interlayer to form a reaction layer of SiC where nucleation should be much less of a problem. Unfortunately, coatings produced in this fashion were still very coarse grained and nodular, and therefore the technique was not pursued further.

Since fine-grained coatings are desirable for this application, other potential causes of the coarse, nodular coatings are currently being investigated. These causes include metallic contamination from the gas

M21718 M21720

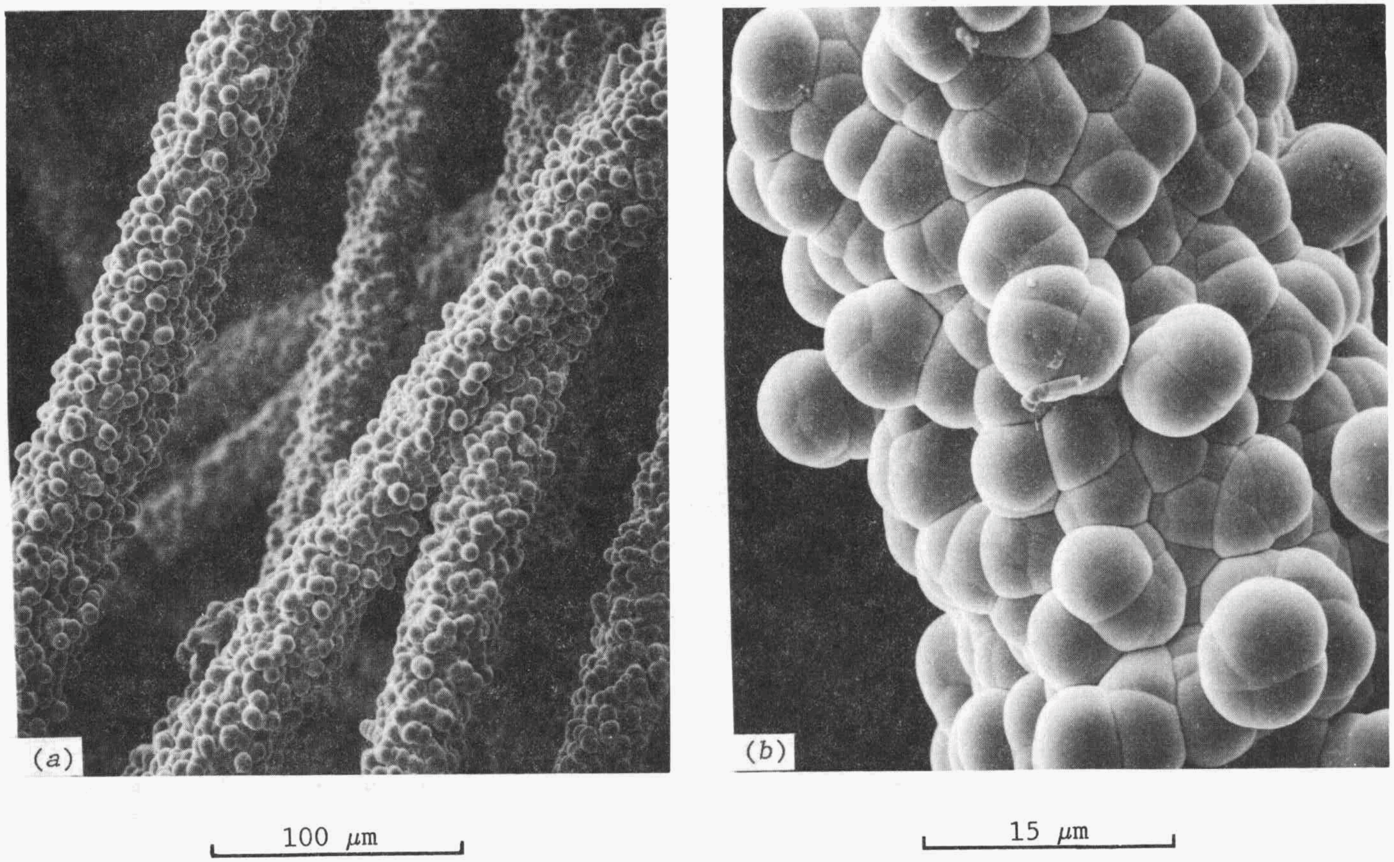

Fig. 8. Microstructure of typical filters showing nodular appearance of the coating; (*a*) and (*b*) nodular coating where individual agglomerates have not grown together, and (*c*) and (*d*) nodular coating where agglomerates have grown together to form a smoother coating.

M21847 M21853

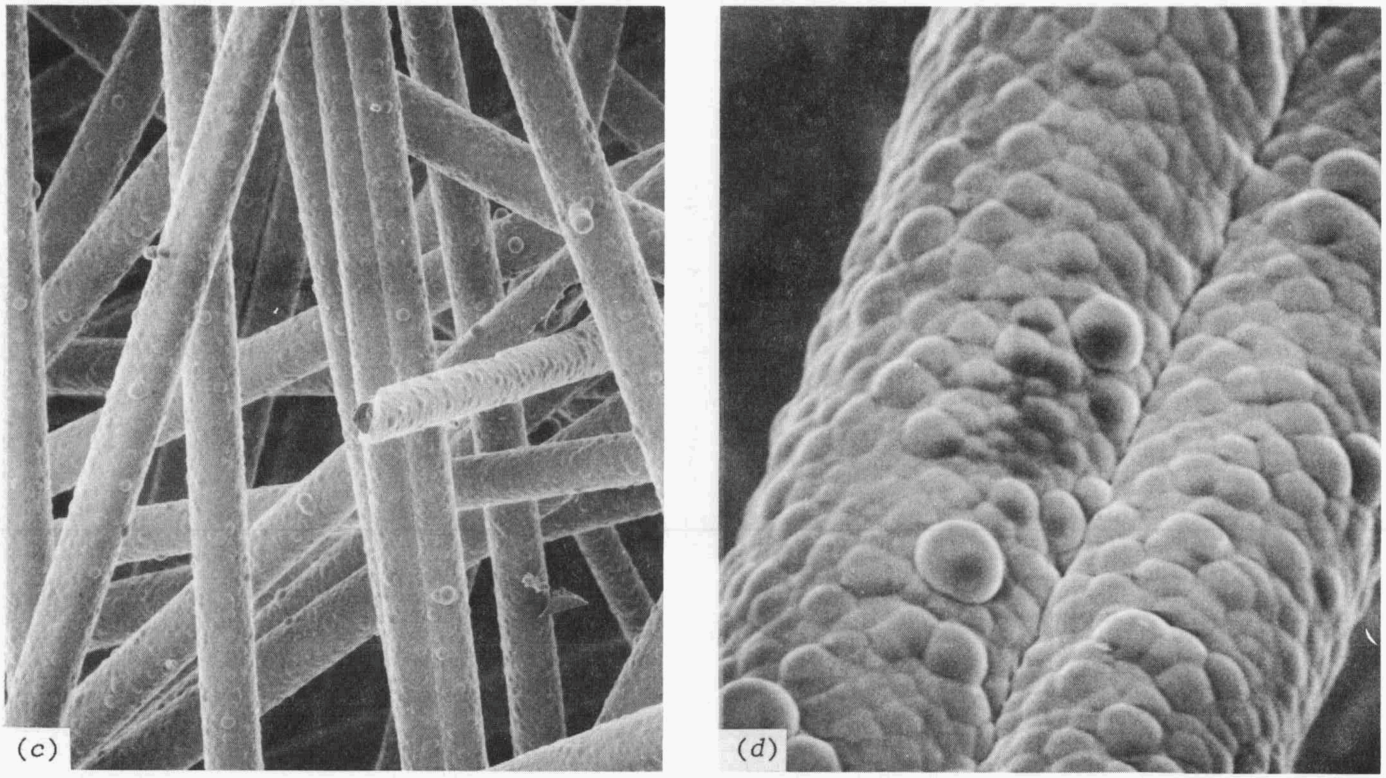

100 μm 15 μm

Fig. 8. Continued.

supply system or furnace components (graphite) that results in whisker formation. Other causes are a minor inleakage of air or homogeneous nucleation in the gas phase resulting in the deposition of SiC agglomerates. The current coatings, even though less than optimum for the filter application, were evaluated so that the characterization techniques would be fully developed when acceptable coatings are obtained.

Initially, filter specimens with varying coating thicknesses were evaluated for mechanical strength. Lightly coated filters (<1 μm) produced the results shown in Fig. 9. Displacement at the center of the filter was observed immediately when the pressure against the neoprene disk was increased. Displacement-pressure curves for these filters are identical to curves obtained when the neoprene disk was tested without a filter specimen. The thin layer of deposited silicon carbide was insufficient to bond one fiber to another. Therefore, as the pressure increased the filter immediately flexed. Filters coated in this fashion might be protected from corrosion; however, they likely have inadequate strengths and would probably suffer from low filter efficiency because of pinholing that results from fiber movement. Thicker coatings are probably required to insure adequate protection from corrosion.

ORNL-DWG 89-8944

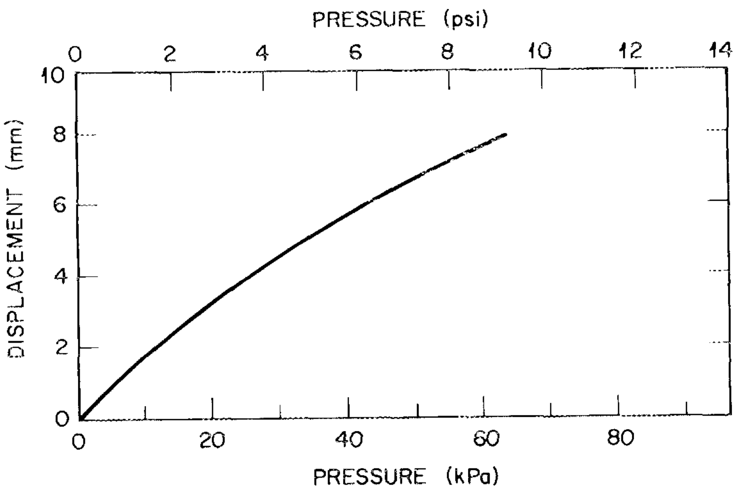

Fig. 9. Strength test results of a lightly coated filter.

Heavily coated filters (>20 μm) behaved very differently as depicted in Fig. 10. As the pressure increased against the neoprene disk, no displacement occurred until very high loads. As the pressure approaches 90 KPa (13 psi), the very thick coatings joining the fibers begin to rupture. The force on the individual fibers at that point is so great that the fibers also rupture. Unfortunately, a large number of fibers rupture in a very short period of time, resulting in very rapid displacement and catastrophic failure of the filters. The slope of the displacement-pressure curve decreases at about 96.6 KPa (14 psi) because the load is carried entirely by the neoprene disk. Heavily coated filters would be very rigid, be protected from corrosion, and have high filtering efficiency; however, they would fail in a brittle fashion if damaged during installation or use.

ORNL-DWG 89-8942

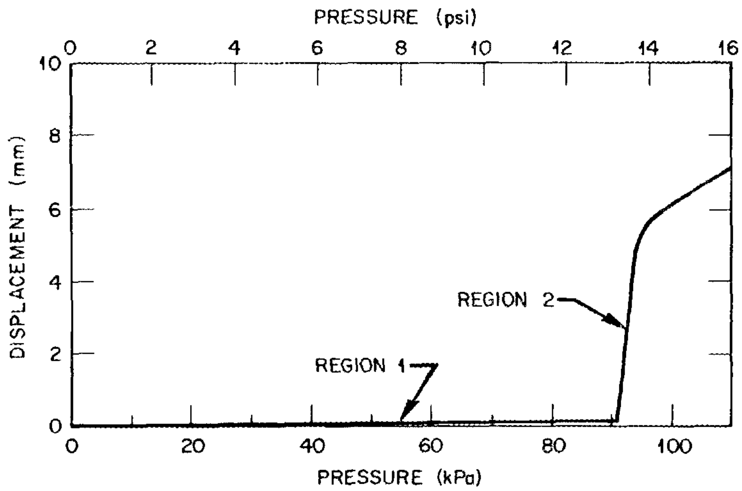

Fig. 10. Strength test results of a heavily coated filter.

A pressure-displacement curve for a filter specimen with a coating thickness of about 5 μm is shown in Fig. 11. This curve can be divided into two distinct regions before failure. Region 1 shows no displacement as the pressure increased in the manner of heavily coated filters. As the

ORNL-DWG 89-8943

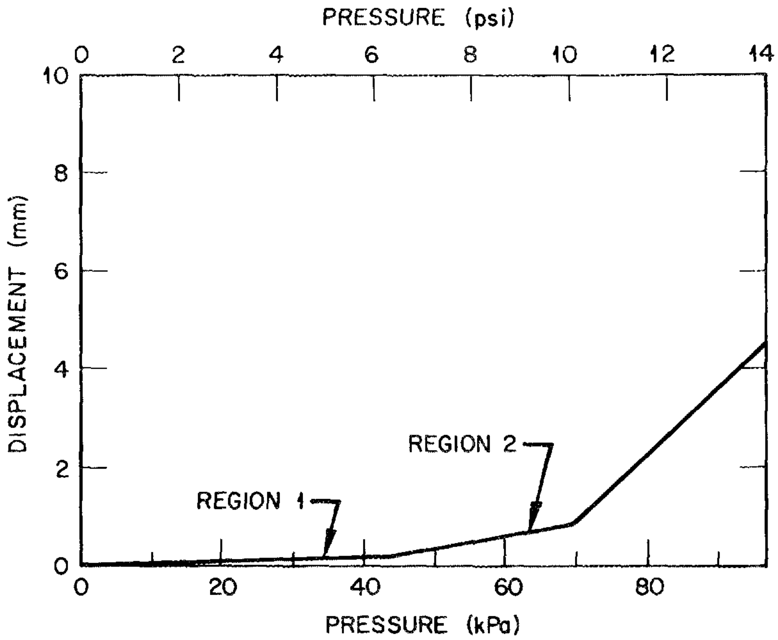

Fig. 11. Strength test results for appropriately coated filter.

pressure approaches 41.4 KPa (6 psi), the coating joining the fibers begins to rupture. Fortunately, the strength of the fibers is sufficient to carry the load; however, the filter begins to flex (region 2). As the load is increased in region 2, more and more fibers separate and the filter shows more and more displacement. Complete failure is evident at about 69.0 KPa (10 psi) where the slope increases to that for a neoprene disk without a filter present. Fractured coatings are evident in the scanning electron micrograph of a failed filter specimen (Fig. 12). Note that the SiC coating fractured, but the Nicalon fiber remained intact. As the load increases, the tensile strength of the fibers is exceeded and fibers begin to break. The filter then fails as indicated by a rapid increase in displacement. Intermediate coating thicknesses (2 to 5 μm) not only protect the filters from corrosion and securely interconnect the fibers, but also show considerable damage tolerance. That is, the fibers slip within the ceramic overcoat, resulting in flexing of the filters. If the fibers were unable to slip within the coating, cracks in the coating would propagate through the fibers, resulting in brittle failure.

M21675

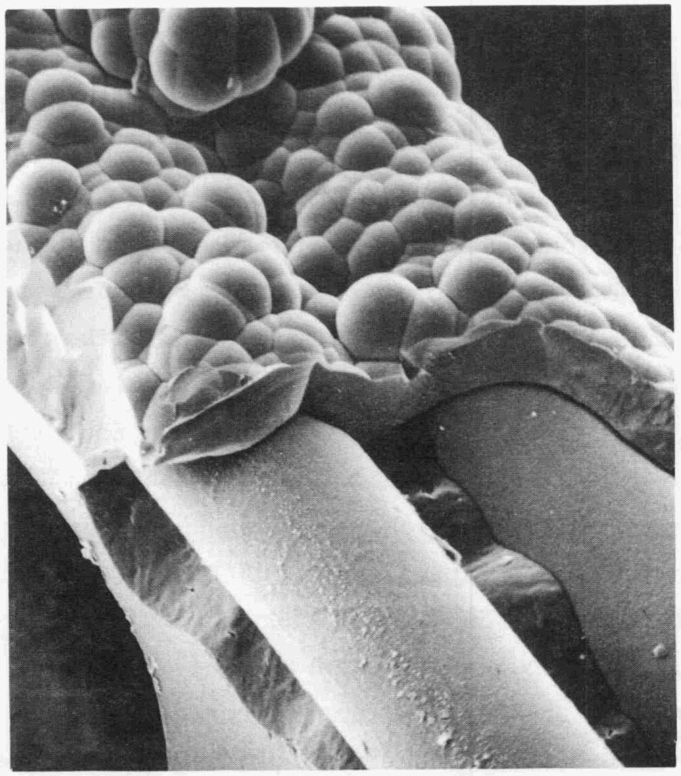

15 μm

Fig. 12. Scanning electron micrograph showing a failed filter with cracked coatings but intact fibers.

The remainder of the filters to be evaluated for mechanical properties in this study were fabricated with very similar SiC deposition conditions described previously. About half the SiC coatings were deposited directly onto the pyrocarbon interlayer and the other half were deposited onto a graded interlayer as described previously. There did not appear to be any correlation between the type interlayer used and the resulting coating morphology. Despite the fact that the deposition conditions were similar for these runs, the microstructure varied considerably from one run to another. The variation in microstructure clearly indicates that the process is not yet reproducible. Apparently, the coating morphology is influenced by contaminants present in the graphite, uncontrolled inleakage of air or oxygen, homogeneous nucleation, or some other unknown variable. Unfortunately, these variables do not remain constant, but fluctuate sufficiently to cause significant variation in the morphology from one coating to the next.

The mechanical strengths were measured on a large number of filters that had coating thicknesses that produced acceptable damage tolerance as described above (Table 1). The coating thicknesses were calculated from the initial filter weight (equivalent length of fiber) and the weight gain due to the coating. The coating thickness calculated from weight gain varied from 1.53 to 3.45 μm and agreed within a factor of 2 for the thickness observed by scanning electron microscopy. The burst strengths, defined as the pressure at which deflection becomes characteristic of the neoprene diaphragm only, varied from 23.4 to 82.8 KPa (3.4 to 12.0 psi) due to the thickness and quality of the coatings. The average strength of these 20 filters was 52.4 $\pm$ 12.9 KPa (7.60 $\pm$ 1.87 psi).

The burst strengths of the flat filter disks are probably somewhat lower than tubular filters because displacement at the center of the disk results in tensile stresses. For normal cylindrical filters, particulate-laden gases would flow from the outer surface toward the center of the tube, putting the filter in compression. Filters should only experience tensile stresses, where they are most susceptible to failure, during the very short periods of pressure pulse cleaning. Furthermore, industrial filters will most likely be folded or corrugated into a four- or five-pointed star to increase the surface area (Fig. 13). Corrugated filters fabricated at ORNL appeared to be stronger and more rigid during handling than cylindrical filters or flat filter disks.

Mechanical strengths were measured for filters that had been thermally cycled (500 to 1100 K) 20 times and 100 times (Table 1). After thermal cycling the filters were examined by scanning electron microscopy for evidence of thermal shock damage. No broken or cracked coatings could be found on the thermally cycled filters. Therefore, the thermal cycling appeared to have no apparent effect on the filter specimens. This was verified by measuring the mechanical strength of thermally cycled filters. The average strength of 12 thermally cycled filters was 47.4 $\pm$ 12.9 KPa

Table 1. Mechanical strengths of filter disks

Run number	Coating thickness from weight gain (μm)	As-coated failure strength [KPa (psi)]	Strength[a] after thermal cycling [KPa (psi)]	Microstructural observations
75	2.32	48.3 (7.0)		Continuous agglomerates[b]
		58.6 (8.5)		Continuous agglomerates
69	2.98	37.9 (5.5)		Loosely packed agglomerates[c]
		45.5 (6.6)		Loosely packed agglomerates
41	2.82	55.2 (8.0)		Continuous agglomerates
		52.4 (7.6)		Continuous agglomerates
52	3.00	73.1 (10.6)		Loosely packed agglomerates
		46.9 (6.8)		Loosely packed agglomerates
61	2.67	82.8 (12.0)	58.6 (8.5)	Loosely packed agglomerates
45	3.20	66.2 (9.6)	37.9 (5.5)	Loosely packed agglomerates
49	2.18	45.5 (6.6)	44.8 (6.5)	Loosely packed agglomerates/ whiskers
57	2.51	52.4 (7.6)	41.4 (6.0)	1-μm coat + dispersed agglomerates
65	3.45	64.1 (9.3)	55.2 (8.0)	Fine-grained coating
46	2.73	50.3 (7.3)	41.4 (6.0)	Continuous agglomerates
51	1.85	58.6 (8.5)	75.9 (11.0)	0.3-μm coating + whiskers
44	2.21	57.2 (8.3)	53.1 (7.7)	Loosely packed agglomerates
40	2.03	43.4 (6.3)	55.2 (8.0)	Loosely packed agglomerates
56	2.14	50.3 (7.3)	44.1 [d](6.4)	Continuous agglomerates
76	1.53	23.4 (3.4)	22.1 [d](3.2)	Loosely packed agglomerates/ whiskers
32	2.05	35.9 (5.2)	40.0 [d](5.8)	0.3 μm coating + whiskers

[a]Each filter was thermally cycled 20 times unless noted.

[b]Continuous agglomerates - coating appears as if it were formed by fusing together 1 to 2 μm spherical agglomerates into a continuous coating, as shown in Fig. 8(*d*).

[c]Loosely packed agglomerates - coating appears as if it were formed by 1 to 2 μm agglomerates but the agglomerates never fused into a continuous coating. Gaps between the agglomerates seem to penetrate a considerable distance into the coating, as shown in Fig. 8(*b*).

[d]Thermally cycled 100 times.

(6.88 ± 1.86 psi), similar to that for as-coated filters. In addition, there was no observable difference between filters thermally cycled 20 times and those thermally cycled 100 times. Cyclic loading at room temperature of filter specimens coated with about 5 μm of SiC produced the results shown in Fig. 14(*a*). No displacement was observed when the pressure was increased to 41.4 KPa (6 psi) (or to any pressure that does not cause cracking of the silicon carbide coating) and held for 1 min.

ORNL-DWG 88-10426

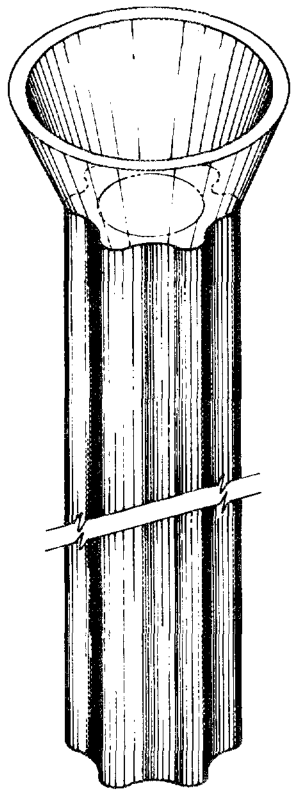

Fig. 13. Schematic drawing of a corrugated candle filter.

After rapidly reducing the load to zero, the pressure was again gradually increased to 41.4 KPa (6 psi). The trace of the second cycle was identical to the trace of the first cycle. The filter was loaded 100 times and the trace of the 100th cycle was identical to the trace of the first cycle. Obviously, the repeated loading at room temperature had no effect on the strength of the filters. Manual operation of the equipment limited the number of cycles that could be easily performed to about 100. Because of the neoprene diaphragm, the test cannot be performed at the normal operating temperature of 1073 K.

In further tests, cyclic loading was increased to a pressure above that which causes cracking. This pressure could be identified because the cracking of the coatings could easily be heard by the operator. The

ORNL-DWG 89-8945

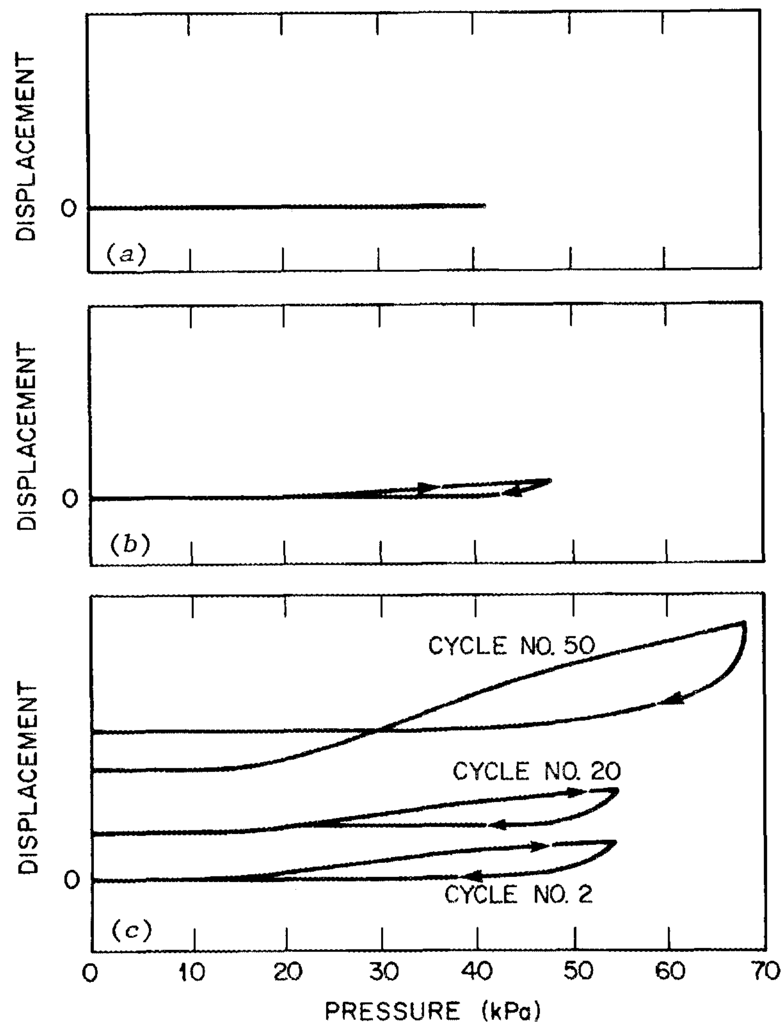

Fig. 14. Effect of pressure cycling on disk-shaped filter specimens.

technique used to measure displacement was not sufficiently precise to detect the cracking of coatings. During the first cycle, the pressure was increased to 41.4 KPa (6 psi) with no displacement. However, as the pressure was increased to 48.3 KPa (7 psi), cracking of the coatings could be heard and the filter flexed slightly. As the pressure was relieved, the displacement dropped rapidly to zero. Repeated cycling of the filter to 48.3 KPa (7 psi) resulted in no audible cracking or further displacement. Figure 14(*b*) shows a typical trace of the displacement-pressure curves which remained unchanged for cycles 2 through 100. The loading curve for the first cycle is described above and coincides with the unloading curve for cycles 2 through 100 in Fig. 14(*b*).

Higher loading [55.2 KPa (8 psi)] resulted in greater displacements that were no longer recoverable. Each cycle to 55.2 KPa (8 psi) resulted in a constant amount of permanent displacement [Fig. 14(*c*)]. As the pressure was increased to 69.0 KPa (10 psi), the amount of displacement that was experienced on each cycle increased until the filter showed complete failure (a rate of displacement equal to that of the unrestrained neoprene disk).

CONCLUSIONS

Testing of fiber-reinforced hot-gas filters revealed that SiC coating thicknesses must be controlled to obtain acceptable mechanical behavior. Thin coatings failed to bond the fibers together, resulting in weak filters that flexed uncontrollably under pressure. These filters might be protected from corrosion but would probably suffer pinhole failure (unacceptable filter efficiency) because of fiber movement and may have inadequate strengths to support the weight of the filtercake. Thick coatings bond fibers together but fail in a brittle manner. Fracture in heavily coated filters results in cracks propagating uncontrollably through both the coatings and the fibers yielding brittle failure. Coatings in the range of 2 to 5 μm are required for appropriate behavior. For properly coated filters, the felt is made rigid and shows no displacement under pressures normally occurring in candle filter systems. Moderate overloading results in cracking of the coating and slight flexing of the filters, but the filter remains functional and intact.

Thermal cycling between 500 and 1100 K had no apparent effect on the mechanical behavior of the fiber-reinforced filters. Since the thermal cycling was not severe enough to cause cracking of the coatings, it was not surprising to see mechanical strengths equal to those of as-coated filters. Repeated cycling of the filters to pressures below that which caused cracking of the coatings had no effect on the mechanical behavior. Filters cycled to pressures that caused limited damage to the coatings also showed no permanent displacement.

The currently produced fiber-reinforced filter material appears promising for particulate removal in fossil energy systems because of its excellent filtering efficiency and good mechanical properties. The results indicate fiber-reinforced filters could continue to be used even after minor damage has occurred. For example, a local overstress in the form of an unusually severe thermal shock, an unusually high pressure drop experienced during cleaning or during use, or mishandling during installation damages the filter by fracturing the ceramic overcoat. Because the stress was insufficient to fracture the ceramic fibers, the filter can operate in a normal fashion. That is, as the load is increased to the normal operating pressure, the filter flexes slightly but controllably. When the load is reversed during the next cleaning or filtering cycle the filter returns to its original shape (the displacement disappears).

ACKNOWLEDGMENTS

The authors appreciate the efforts of C. H. Hsueh and J. I. Federer for technical review, C. A. Valentine for preparing the draft report, P. H. Miller for editing assistance, and B. Q. Atkinson for preparing the manuscript for publication. We are particularly grateful to J. I. Federer for helpful discussions over the past year concerning sodium corrosion of ceramics.

REFERENCES

1. Sawyer, J., *Assessment of the Causes of Failure of Ceramic Filters for Hot-Gas Cleanup in Fossil Energy Systems and Determination of Materials Research and Development Needs*, ORNL/Sub/86-57964/01, January 1989.

2. Mah, T., et al., "Thermal Stability of SiC Fibers," *J. Mater. Sci.* **19**, 1191-201 (1984).

3. Smialek, J. L., and Jacobson, N. S., "Mechanism of Strength Degradation for Hot Corrosion of α-SiC," *J. Am. Ceram. Soc.* **69**(10), 741-52 (1986).

4. Jacobson, N. S., and Fox, D. S., "Molten-Salt Corrosion of Silicon Nitride: II, Sodium Sulfate," *J. Am. Ceram. Soc.* 71(2), 128–48 (1988).

5. Federer, J. I., "Corrosion of SiC Ceramics by Na_2SO_4," *Adv. Ceram. Mater.* 3(1), 56–61 (January 1988).

6. Richerson, D. W., *Modern Ceramic Engineering: Properties, Processing, and Use in Design*, Marcel Dekker, Inc., New York, 1982, p. 126.

7. Brown, N., Virginia Polytechnic Institute and State Univ., Blacksburg, VA, personal communication to D. P. Stinton, February 22, 1989.

8. Brown, J. J., Virginia Polytechnic Institute and State Univ., Blacksburg, VA, personal communication to D. P. Stinton, February 22, 1989.

9. Brittain, R., SRI International, Menlo Park, CA, personal communication to D. P. Stinton, February 22, 1989.

10. Stinton, D. P., and Lowden, R. A., "Fabrication of Fiber-Reinforced Hot-Gas Filters By CVD Techniques," *Ceram. Eng. Sci. Proc.* 9(9–10), 1233–44 (1988).

11. Kingery, W. D., Bowen, H. K., and Uhlmann, D. R., *Introduction to Ceramics*, John Wiley & Sons, New York, 1976, p. 811.

12. Rice, R. W., "Mechanisms of Toughening in Ceramic Matrix Composites," *Ceram. Eng. Sci. Proc.* 2(7–8), 661–701 (1981).

13. Drenker, S. G., Electric Power Research Institute, Palo Alto, CA, personal communication to D. P. Stinton, February 17, 1989.

14. Lowden, R. A., and Stinton, D. P., *The Influence of the Fiber-Matrix Bond on the Mechanical Behavior of Nicalon/SiC Composites*, ORNL/TM-10667, December 1987.

15. Stinton, D. P., "Ceramic Composites By Chemical Vapor Infiltration," pp. 1028–40 in *Proc. Tenth Int'l Conf. Chem. Vapor Dep.*, ed. G. W. Cullen and J. M. Blocher, Jr., Electrochem. Society, Pennington, NJ, 1987.

16. Lowden, R. A., Stinton, D. P., and Besmann, T. M., "Characterization of Fiber-Matrix Interfaces in Ceramic Composites," pp. 1028–40 in *Whisker- and Fiber-Toughened Ceramics, Proceedings of an International Conference*, ed. R. A. Bradley, D. E. Clark, D. C. Larsen, and J. O. Stiegler, ASM International, Honolulu, Hawaii, October 18–23, 1987.

17. Stinton, D. P. and Chang, R., *Ceramic-Fiber Ceramic-Matrix Hot-Gas Filters*, DOE/METC-87/6079, Vol. 1, Morgantown Energy Technology Center, Morgantown, WV, June 1987.

18. Bunshah, R. F., *Deposition Technologies for Films and Coatings*, ed. R. F. Bunshah et al., Noyes Publications, Park Ridge, NJ, 1982.

19. Thornton, J. A., "High Rate Thick Film Growth," *Ann. Rev. Mater. Sci.* 7, 239–60 (1977).

INTERNAL DISTRIBUTION

1–2. Central Research Library
3. Document Reference Section
4–5. Laboratory Records Department
6. Laboratory Records, ORNL RC
7. ORNL Patent Section
8–10. M&C Records Office
11. P. Angelini
12. R. L. Beatty
13. T. M. Besmann
14. P. J. Blau
15. A. Bleier
16. R. A. Bradley
17. D. N. Braski
18. P. T. Carlson
19. D. F. Craig
20–24. D. Dellinger
25. J. I. Federer
26. H. M. Henson
27. R. S. Holcomb
28. C. Hsueh
29. T. J. Huxford
30. R. R. Judkins
31. M. A. Karnitz
32. R. T. King
33. E. L. Long, Jr.
34–38. R. A. Lowden
39. J. P. Moore
40–44. L. Riester
45. P. L. Rittenhouse
46. A. F. Rowcliffe
47. A. C. Schaffhauser
48. V. K. Sikka
49. B. W. Sheldon
50–74. D. P. Stinton
75. R. W. Swindeman
76. T. N. Tiegs
77. A. C. Young
78. A. D. Brailsford (Consultant)
79. H. D. Brody (Consultant)
80. F. F. Lange (Consultant)
81. D. P. Pope (Consultant)
82. E. R. Thompson (Consultant)
83. J. B. Wachtman (Consultant)

EXTERNAL DISTRIBUTION

84–85. ACUREX CORPORATION, 555 Clyde Avenue, P.O. Box 7555, Mountain View, CA 94039

J. Sawyer
J. J. Schaefer

86. ADIABATICS, INCORPORATED, 630 South Mapleton, Columbus, IN 47201

R. Kamo, President

87. ADVANCED COMPOSITE MATERIALS CORPORATION, 1525 South Buncombe Road, Greer, SC 29651

J. F. Rhodes

88–90. AFWAL/MLLM, Wright-Patterson AFB, OH 45433

A. Katz
L. Matson
S. Szaruga

91–94. AIR PRODUCTS AND CHEMICALS, INC., P.O. Box 538T, Allentown, PA 18105

P. N. Dyer
V. L. Magnotta
R. K. Malhotra
S. V. Raman

95. AIRCO TEMESCAL, 2850 Seventh Street at Heinz, Berkeley, CA 94710

E. Demiray

96. AIRESEARCH MANUFACTURING COMPANY, 2525-T West 190th Street, Torrance, CA 90509

D. M. Kotchick

97. ALFRED UNIVERSITY, New York State College of Ceramics, Center for Advanced Ceramic Technology, Alfred, NY 14802

R. M. Spriggs

98–99. AMERCOM, INC., 8928 Fullbright Avenue, Chatsworth, CA 91311

C. V. Burkland
W. E. Bustamante

100–101. AMERICAN MATRIX, INC., 118 Sherlake Drive, P.O. Box 23556, Knoxville, TN 37933

R. Nixdorf
S. Weaver

102–103. ARGONNE NATIONAL LABORATORY, 9700 South Cass Avenue, Argonne, IL 60439

W. A. Ellingson
J. P. Singh

104–105. ARMY MATERIALS TECHNOLOGY LABORATORY, 405 Arsenal Street, Watertown, MA 02172

R. N. Katz
J. W. McCauley

106. AVCO, 201 Lowell Street, Wilmington, MA 01887

T. Vasilos

107–108. AVCO LYCOMING, 550 Main Street, Stratford, CT 06497

S. Naik
T. M. Pattison

109–112. AVCO SPECIALTY MATERIALS, 2 Industrial Avenue, Lowell, MA 01851

B. Belason
T. F. Foltz
W. Foulds
J. F. LeCostaouec

113–117. BABCOCK & WILCOX COMPANY, Lynchburg Research Center, P.O. Box 239, Lynchburg, VA 24505

L. J. Ferrell
W. G. Long
H. H. Moeller
W. Parks
R. Ramey

118–119. BASIC INDUSTRY RESEARCH LABORATORY, 1801 Maple Avenue, Evanston, IL 60201-3135

J. W. Cox
R. R. Fessler

120–122. BATTELLE COLUMBUS LABORATORIES, 505 King Avenue, Columbus, OH 43201

K. F. Dufrane
S. P. Mukherjee
I. G. Wright

123–126. BATTELLE PACIFIC NORTHWEST LABORATORIES, P.O. Box 999, Battelle Boulevard, Richland, WA 99352

E. Cartwright
T. D. Chikalla
S. D. Dahlgren
E. McClanahan

127–131. CATERPILLAR, INC., Technical Center, P.O. Box 1875, Peoria, IL 61656-1875

D. Beahler
M. Haselkorn
F. Kelly
G. G. Valbert
C. D. Weiss

132–133. CERAMATEC, INC., 163 West 1700 Street, Salt Lake City, UT 84115

C. W. Griffin
D. W. Richerson

134. COMURHEX, INC., Usine de Pierrelatte, B.P. 29 - 26701, Pierrelatte, Cedex, France

D. Gaillard

135. COORS CERAMICS COMPANY, Research and Development, Turbine Programs and Heat Exchangers, 17750 West 32nd Street, Golden, CO 80401

R. Kleiner, Manager

136-139. CORNING GLASS WORKS, Corning, NY 14831

K. Chyung
R. C. Doman
D. C. Larson
P. Papa

140-143. CUMMINS ENGINE COMPANY, INC., 1000 5th Street, Columbus, IN 47201

M. Naylor
J. W. Patten
G. L. Starr
T. M. Yonushonis

144. DFVLR GERMAN AEROSPACE RESEARCH ESTABLISHMENT, Materials Laboratory, D-5000, Koln 90, Federal Republic of Germany

W. Bunk

145-147. DOW CORNING CORPORATION, 3901 South Saginaw Road, Midland, MI 48640

H. W. Foglesong
R. E. Jones
D. R. Petrak

148. DREXEL UNIVERSITY, Department of Materials Engineering, Fibrous Materials Research Center, Philadelphia, PA 19104

F. K. Ko

149. DUPONT LANXIDE COMPOSITES, INC., One Tralee Industrial Park, Newark, DE 19714

J. E. Garnier

150-155. E. I. DUPONT DE NEMOURS & COMPANY, INC., Pencader Plant, Composites Division, Diamond State Industrial Park, Newark, DE 19713

P. Geoghegan
P. E. Gray
M. H. Headinger
C. Lundgren
J. Morris
J. C. Romine

156-157. ELECTRIC POWER RESEARCH INSTITUTE, 3412 Hillview Avenue, P.O. Box 10412, Palo Alto, CA 94303

R. Chang
S. G. Drenker

158-161. ENGELHARD CORPORATION, Menlo Park, CN 28, Edison, NJ 08818

M. Gershesb
A. Mishra
K. E. Voss
B. Yavuz

162-163. FORD MOTOR COMPANY, Engineering and Research, P.O. Box 2053, Dearborn, MI 48121

G. M. Crosbie
D. L. Hartsock

164-165. GENERAL ATOMICS, P.O. Box 81608, San Diego, CA 92138

T. D. Gulden
K. S. Mazdiyasni

166. GENERAL MOTORS CORPORATION, Allison Gas Turbine Operations, Low Heat Rejection Diesel Technology, P.O. Box 420, Indianapolis, IN 46206

H. E. Helms

167-169. GEORGIA TECH RESEARCH INSTITUTE, Energy and Materials Sciences Laboratory, Atlanta, GA 30332

J. A. Hanigofsky
W. J. Lackey
T. L. Starr

170-174. GTE LABORATORIES, INC., 40 Sylvan Road, Waltham, MA 02254

M. L. Huckabee
H. J. Kim
A. E. Pasto
H. E. Rebenne
V. Sarin

175. HUGHES AIRCRAFT COMPANY, P.O. Box 902, 2000 East El Segundo Boulevard, El Segundo, CA 90245

M. Gardos

176. KAMAN SCIENCES CORPORATION, 1500 Garden of the Gods Road, P.O. Box 7463, Colorado Springs, CO 80933

J. L. Carr

177–178. KENNAMETAL, INC., P.O. Box 231, Latrobe, PA 15650

D. Kropful
E. J. Oles

179. KRW ENERGY SYSTEMS, P.O. Box 158, Madison, PA 15663

C. A. Andersson, Jr.

180–182. LANXIDE CORPORATION, Tralee Industrial Park, Newark, DE 19711

V. Irick, Jr.
M. Newkirk
A. W. Urquhart

183–185. LAWRENCE BERKELEY LABORATORY, University of California, P.O. Box 808, One Cyclotron Road, Berkeley, CA 94720

D. H. Boone
L. C. DeJonghe
A. V. Levy

186–188. LOS ALAMOS NATIONAL LABORATORY, P.O. Box 1663, Los Alamos, NM 87545

F. D. Gac
G. F. Hurley
J. J. Petrovic

189. MAN TECHNOLOGIE GmbH, Postfach 50 04 26, Dachauer Strasse 667, D-8000 Munchen 50, Federal Republic of Germany

A. Muehlratzer

190–191. MARTIN MARIETTA LABORATORIES, 1450 South Rolling Road, Baltimore, MD 21227

D. C. Nagle
A. R. C. Westwood

192–193. MASSACHUSETTS INSTITUTE OF TECHNOLOGY, Cambridge, MA 02139

H. K. Bowen
J. S. Haggerty

194–195. MECHANICAL TECHNOLOGY, INC., 968 Albany-Shaker Road, Latham, NY 12110

W. F. Bessler
M. Schreiner

196. NASA-LANGLEY RESEARCH CENTER, MS 188-B, Hampton, VA 23665

D. R. Tenney

197–202. NASA-LEWIS RESEARCH CENTER, 21000 Brookpark Road, Cleveland, OH 44135

C. C. Berndt
D. H. Buckley
S. R. Levine
T. J. Miller
H. B. Probst
H. Sliney

203–204. NATIONAL INSTITUTE OF STANDARDS AND TECHNOLOGY, 562 Fracture and Deformation, Gaithersburg, MD 20899

E. R. Fuller
S. M. Wiederhorn

205–206. NATIONAL RESEARCH COUNCIL OF CANADA, 1411 Oxford Street, Halifax, N.S., Canada B3H3Z1

S. Karunanithy
K. J. Konsztowicz

207–209. NAVAL SURFACE WARFARE CENTER, Code R31, 10901 New Hampshire Avenue, Silver Spring, MD 20903-5000

D. Hought
C. A. Martin
E. Wuchina

210. NEW MEXICO INSTITUTE OF MINING AND TECHNOLOGY, Department of Materials and Metallurgical Engineering, Socorro, NM 87801

K. K. Chawla

211–212. NORTH CAROLINA STATE UNIVERSITY, Department of Materials Engineering, P.O. Box 5427, 232 Riddick Laboratory, Raleigh, NC 27607

H. Conrad
R. F. Davis

213–214. NORTH CAROLINA A&T STATE UNIVERSITY, Greensboro, NC 27411

A. D. Kelkar
J. Sankar

215. NORTH CAROLINA STATE UNIVERSITY, P.O. Box 5995, Raleigh, NC 27607

H. Palmour III

216. NORTHWESTERN UNIVERSITY, The Technological Institute, Department of Materials Science and Engineering, Evanston, IL 60208

K. T. Faber

217. OAK RIDGE ASSOCIATED UNIVERSITIES LIBRARY, Oak Ridge, TN 37831

MERT Division

218. OHIO STATE UNIVERSITY, 2041 College Road, Columbus, OH 43210

D. Readey

219–220. PENNSYLVANIA STATE UNIVERSITY, Materials Engineering Research Laboratory, 201 Steidle Building, University Park, PA 16802

K. Spear
R. E. Tressler

221–223. PRATT & WHITNEY AIRCRAFT, 400 Main Street, East Hartford, CT 06108

O. Chen
C. S. Giggins
D. L. Ruckle

224. REFRACTORY COMPOSITES, INC., 12220-A Rivera Road, Whittier, CA 90606

E. Paquette

225. ROCKWELL INTERNATIONAL, 1049 Camino Dos Rios, P.O. Box 1085, Thousand Oaks, CA 91360

P. E. D. Morgan

226. SANDIA NATIONAL LABORATORIES, P.O. Box 5800, Albuquerque, NM 87115

D. Maddox

227. R. L. Smith, P.O. Box 98, Chassel, MI 49916

228–229. SOLAR TURBINES, INC., 2200 Pacific Highway, P.O. Box 85376, San Diego, CA 92138-5376

A. Hasen
M. Van Roode

230. TECHNOLOGY ASSESSMENT AND TRANSFER COMPANY, 9607 Muirfield Drive, Upper Marlboro, MD 20772

L. L. Fehrenbacher

231–236. 3M COMPANY, 3M Center, 218-35-04, St. Paul, MN 55144

J. Copes
E. Funkenbusch
T. Kafka
M. A. Leitheiser
R. E. Richards
L. White

237. UNION CARBIDE CORPORATION, Market Development, Carbon Products Division, P.O. Box 6087, Cleveland, OH 44101

M. B. Dowell

238. U.S. ARMY TANK-AUTOMOTIVE COMMAND (TACOM), R&D Center, Warren, MI 48090

P. C. Glance

239. U.S. DEPARTMENT OF DEFENSE, Advanced Research Projects Agency, 1400 Wilson Boulevard, Arlington, VA 22209

B. F. Wilcox

240-241. UNITED TECHNOLOGIES RESEARCH CENTER, Silver Lane, MS 24, East Hartford, CT 06108

J. J. Brennan
K. Prewo

242. UNIVERSITY OF CALIFORNIA, College of Engineering, Santa Barbara, CA 93106

A. G. Evans

243. UNIVERSITY OF CALIFORNIA AT BERKELEY, Department of Materials Science and Mineral Engineering, Hearst Mining Building, Berkeley, CA 94720

J. W. Evans

244. UNIVERSITY OF DELAWARE, Center for Composite Materials, 228 Spencer Laboratory, Newark, DE 19716

T. W. Chou

245. UNIVERSITY OF NEWCASTLE UPON TYNE, Department of Metallurgy and Engineering Materials, Newcastle upon Tyne, NE1 7RU, England

T. F. Page

246. UNIVERSITY OF TENNESSEE, Department of Materials Science, Knoxville, TN 37996

J. E. Spruill

247. UNIVERSITY OF WASHINGTON, Seattle, WA 98195

R. C. Bradt

248-252. VIRGINIA POLYTECHNIC INSTITUTE AND STATE UNIVERSITY, Blacksburg, VA 24061

J. J. Brown, Jr.
D. P. H. Hasselman
K. L. Reifsnider
W. W. Stinchcomb
R. E. Swanson

253. VOUGHT CORPORATION, MSTH 83, P.O. Box 225907, Dallas, TX 75265

H. F. Volk

254-255. W. R. GRACE & COMPANY, 7379 Route 32, Columbia, MD 21044

W. R. Rice
J. P. Skalny

256. WESTINGHOUSE ELECTRIC CORPORATION, Research and Development Center, 1310 Beulah Road, Pittsburgh, PA 15235

R. J. Bratton

257-258. WILLIAMS INTERNATIONAL CORPORATION, 2280 West Maple Road, Walled Lake, MI 48088

W. Chapman
P. Nagy

259-263. DOE, CONSERVATION AND RENEWABLE ENERGY, Forrestal Building, Washington, DC 20585

A. A. Chesnes, CE-151
J. J. Eberhardt, CE-142
S. L. Richlen, CE-141
R. B. Schulz, CE-151
S. M. Wolf, CE-12

264-274. DOE, MORGANTOWN ENERGY TECHNOLOGY CENTER, P.O. Box 880, Morgantown, WV 26505

R. A. Bajura
R. C. Beddick
J. W. Byam
D. C. Cicero
R. J. Dellefield
R. Dennis
D. Dubis
N. T. Holcombe
W. J. Huber
J. S. Wilson
C. M. Zeh

275. DOE, OFFICE OF BASIC ENERGY SCIENCES, Division of Materials Sciences, ER-131, GTN, Washington, DC 20545

R. J. Gottschall

276-278. DOE, OFFICE OF FOSSIL ENERGY, FE-14, Mail Stop B127, GTN, Washington, DC 20545

D. J. Beecy
J. P. Carr
F. M. Glaser

279. DOE, PITTSBURGH ENERGY TECHNOLOGY CENTER, P.O. Box 10940, Pittsburgh, PA 15236

S. W. Chun

280–281. DOE, OAK RIDGE OPERATIONS, P.O. Box 2001, Oak Ridge, TN 37831-8600

Office of Assistant Manager for Energy Research and Development
E. E. Hoffman

282–291. DOE, OFFICE OF SCIENTIFIC AND TECHNICAL INFORMATION, Office of Information Services, P.O. Box 62, Oak Ridge, TN 37831

For distribution by microfiche as shown in DOE/TIC-4500, Distribution Categories UC-105 (Flue Gas Cleanup), UC-106 (Gas Stream Cleanup), and UC-114 (Coal Based Materials and Components).

☆U.S. GOVERNMENT PRINTING OFFICE 1989—648-119/00029